

# Degradation of brown adipocyte purine nucleotides regulates uncoupling protein 1 activity



Tobias Fromme<sup>1,2,5,\*</sup>, Karin Kleigrewer<sup>3</sup>, Andreas Dunkel<sup>4,5</sup>, Angelika Retzler<sup>4,5</sup>, Yongguo Li<sup>1,2,5</sup>, Stefanie Maurer<sup>1,2,5</sup>, Natascha Fischer<sup>1,2,5</sup>, Rolf Diezko<sup>1</sup>, Timo Kanzleiter<sup>1</sup>, Verena Hirschberg<sup>1</sup>, Thomas Hofmann<sup>3,4,5</sup>, Martin Klingenspor<sup>1,2,5</sup>

## ABSTRACT

**Objective:** Non-shivering thermogenesis in mammalian brown adipose tissue depends on thermogenic uncoupling protein 1. Its activity is triggered by free fatty acids while purine nucleotides mediate inhibition. During activation, it is thought that free fatty acids overcome purine-mediated inhibition. We measured the cellular concentration and the release of purine nucleotide metabolites to uncover a possible role of purine nucleotide degradation in uncoupling protein 1 activation.

**Methods:** With mass spectrometry, purine nucleotide metabolites were quantified in cellular homogenates and supernatants of cultured primary brown adipocytes. We also determined oxygen consumption in response to a  $\beta$ -adrenergic agonist.

**Results:** Upon adrenergic activation, brown adipocytes decreased the intracellular concentration of inhibitory nucleotides (ATP, ADP, GTP and GDP) and released the respective degradation products. At the same time, an increase in cellular calcium occurred. None of these phenomena occurred in white adipocytes or myotubes. The brown adipocyte expression of enzymes implicated in purine metabolic remodeling is altered upon cold exposure. Pharmacological and genetic interference of purine metabolism altered uncoupling protein 1 mediated uncoupled respiration.

**Conclusion:** Adrenergic stimulation of brown adipocytes lowers the intracellular concentration of purine nucleotides, thereby contributing to uncoupling protein 1 activation.

© 2017 The Authors. Published by Elsevier GmbH. This is an open access article under the CC BY-NC-ND license (<http://creativecommons.org/licenses/by-nc-nd/4.0/>).

**Keywords** Purine nucleotides; Uncoupling protein 1; Brown adipose tissue; Non-shivering thermogenesis; HILIC-MS/MS; Guanosine monophosphate reductase

## 1. INTRODUCTION

Mammalian non-shivering thermogenesis in brown adipose tissue is a heat dissipation mechanism of immense specific capacity. As such, it has to be tightly controlled to prevent wasting stored energy reserves. Mitochondrial uncoupling protein 1 (UCP1) is essential for the thermogenic process and a target of the crucial regulatory signals. In the resting state, UCP1 is inhibited by the binding of free (i.e. non-complexed to magnesium or calcium) purine di- and triphosphate nucleotides (GDP, ADP, GTP, ATP). Upon  $\beta$ -adrenergic activation, lipolytically liberated free fatty acids directly interact with UCP1 to overcome inhibition by purine nucleotides (reviewed in [1]).

The cytosolic concentration of free ATP alone (0.25–10 mM) far exceeds its binding constant to UCP1 ( $<1 \mu\text{M}$ ) as determined in proteoliposome experiments [2]. According to the established model of

UCP1 regulation, modulating the concentration of purine di- and triphosphate nucleotides is thus not a means of UCP1 activation.

As already noted by others, this assessment seems inappropriate given the substantial evidence for a flexible, different binding constant of purine nucleotides to UCP1 *in vivo* [3,4]. Firstly, the mitochondrial inner membrane lipid cardiolipin reduces purine nucleotide binding to UCP1 in a dose-dependent manner [3]. At the 12% molar amount cardiolipin expected in BAT mitochondria [5,6], the KD is increased more than 10-fold. Secondly, purine nucleotide inhibition is pH dependent [7]. Upon activation of thermogenesis in a brown fat cell, the cytosolic pH increases to up to 8.0 [8]. In a conservative estimate, in the presence of 12% cardiolipin and at a moderate pH of 7.5, the calculated KD is not  $<1 \mu\text{M}$ , but already as high as  $80 \mu\text{M}$ . Thirdly, the concentration of free nucleotides depends on the concentration of divalent cations in the cytosol [7]. The cytosolic concentrations of calcium and magnesium increase following activation of a brown adipocyte as a consequence of

<sup>1</sup>Chair of Molecular Nutritional Medicine, TUM School of Life Sciences, Technical University of Munich, Germany <sup>2</sup>EKFZ — Else Kröner-Fresenius Center for Nutritional Medicine, Technical University of Munich, Freising, Germany <sup>3</sup>Bavarian Center for Biomolecular Mass Spectrometry (BayBioMS), Technical University of Munich, Freising, Germany <sup>4</sup>Chair of Food Chemistry and Molecular Sensory Science, Technical University of Munich, Freising, Germany <sup>5</sup>ZIEL — Institute for Food & Health, Technical University of Munich, Freising, Germany

\*Corresponding author. Technical University Munich, Chair of Molecular Nutritional Medicine, Gregor-Mendel-Str. 2, 85354 Freising, Germany. E-mail: [fromme@tum.de](mailto:fromme@tum.de) (T. Fromme).

Received November 17, 2017 • Revision received December 11, 2017 • Accepted December 19, 2017 • Available online 26 December 2017

<https://doi.org/10.1016/j.molmet.2017.12.010>

both uptake from the extracellular medium and release from intracellular stores [9–12]. Free purine nucleotide concentrations will decrease accordingly.

For all these reasons, the concentration of purine nucleotides capable of inhibiting UCP1 can be assumed to be well in a range, in which a further degradation may actively contribute to activation of UCP1 and/or sensitize to fatty acid activation. Indeed, brown adipose tissue mRNA and protein abundance of central enzymes of purine nucleotide metabolism are strongly regulated upon cold exposure [13,14].

In this study, we investigated concentration changes of purine nucleotides in activated brown adipocytes by hydrophilic interaction chromatography and mass spectrometry. We found a decrease in purine nucleotide di- and triphosphate concentration upon adrenergic stimulation of primary brown adipocytes and present evidence that alterations in purine nucleotide metabolism are involved in the activation of UCP1-mediated thermogenesis.

## 2. MATERIAL & METHODS

### 2.1. Cell culture and transfection

Primary brown adipocytes were prepared from the interscapular brown adipose tissue of male C57BL/6J mice as previously described [15]. Mice originated from our specific pathogen free barrier colony that operates according to the German Animal Welfare Law.

Proliferating cells were maintained in Dulbecco's modified Eagle medium (DMEM) with 10% fetal bovine serum (FBS). Confluent cells were induced by addition of 0.5 mM isobutylmethylxanthine (IBMX), 125 nM indomethacin, 1  $\mu$ M dexamethasone, 850 nM insulin and 1 nM T3 for 2 days and differentiated for a further 6 days in the presence of 850 nM insulin and 1 nM T3. Immortalized, primary brown adipocytes were a gift from Bruce Spiegelman's lab, generated by a published method [16], and cultured by the above protocol.

3T3-L1 white adipocytes were proliferated in DMEM plus 10% FBS, induced for 3 days in the presence of 5  $\mu$ g/ml insulin, 250 nM dexamethasone and 0.5 mM IBMX, and differentiated for a further 6 days with 5  $\mu$ g/ml insulin. C2C12 myoblasts were proliferated in DMEM plus 10% FBS and differentiated for 8 days in DMEM plus 2% horse serum. Human embryonic kidney cells (HEK293) were cultured in DMEM plus 10% FBS. The generation and validation of HEK293 cells stably expressing UCP1 has been described previously [17]. Transient transfection of a GMPR overexpression plasmid (pCMV-Sport6) was performed by the calcium phosphate method (ProFection Kit, Promega) using 10  $\mu$ g of vector.

We detected cytosolic protease activity in cell culture supernatants as a marker of ruptured cells with a commercial kit system (CytoTox Glo, Promega).

### 2.2. Respirometry

Oxygen consumption of primary brown adipocytes was determined at 37 °C with an XF96 extracellular flux analyzer (Seahorse Bioscience) following a published protocol [18]. Briefly, cells were fully differentiated on appropriate multiwell plates and changed to unbuffered DMEM with 2% bovine serum albumin and a CO<sub>2</sub>-free incubator 1 h before the measurement. ATP synthesis was blocked by injection of 5  $\mu$ M oligomycin A, UCP1 mediated respiration was activated by addition of 0.5  $\mu$ M isoproterenol, maximal respiration by 1  $\mu$ M Carbonyl-cyanide p-[trifluoromethoxy]-phenyl-hydrazone (FCCP) and finally non-mitochondrial respiration by 5  $\mu$ M antimycin A. Results are shown as mean values  $\pm$  SD of 10–12 replicate wells.

Oxygen consumption of HEK293 cells was determined by a Clark-type electrode (Model 10, Rank Brothers Ltd) at 37 °C in DMEM medium.

Cells were trypsinized, pelleted and resuspended in fresh DMEM. After measurement of basal respiration, ATP synthesis was inhibited by 1.2  $\mu$ M oligomycin A and the basal leak was quantified. A bolus of 300  $\mu$ M palmitate was used to activate UCP1-mediated uncoupling and 3  $\mu$ M FCCP to fully uncouple to maximal respiration rate.

### 2.3. Quantitation of purine metabolites, fatty acids and cations

We harvested metabolites by washing cultured cells with ice-cold phosphate buffered saline (pH 7.4), placing the dish on ice and scraping cells in ice-cold 15 mM tetrabutylammonium hydrogen sulfate (TBAHS, pH 2.0) including a 5  $\mu$ M internal standard mix of 15N-labeled ATP, GTP, AMP, GMP (Silantes, Munich, Germany) and 13C-labeled adenosine (Cambridge Isotope Laboratories, Andover, USA). Samples were centrifuged and clear supernatants analyzed by HILIC-MS/MS using a ZIC pHILIC 5  $\mu$ M, 150  $\times$  4.6 mm column (Merck) to quantify nucleotides and by RP-LC-MS/MS using a Synergi Polar-RP 100 A, 2.5  $\mu$ m, 2.0  $\times$  100 mm column (Phenomenex, Aschaffenburg, Germany) to quantify fatty acids (detailed method in the Supplement). Cations were quantified in the same samples by ion exchange chromatography (Chromatograph: Dionex ICS-2000, Thermo Fischer) using Dionex Ion Pac CS19 (Thermo Fisher) column with 0.1 M methanol sulfonic acid as solvent with a 250  $\mu$ L/min flowrate. One brown adipocyte outlier sample was excluded from the divalent cation analysis due to >5-fold content as compared to the next highest sample. This removal had no effect on statistically significant group differences. All analytical data were normalized to DNA concentration measured by bis-benzimide fluorometry as a surrogate measure for cell number.

### 2.4. Transcript quantification

Primer sequences for transcript detection with quantitative PCR are given in Suppl. Table 4. We employed cDNA from a first strand synthesis from total RNA (Quantitect cDNA synthesis Kit, Qiagen) in a qPCR reaction mix including SYBR Green (Sensimix, Bioline) on a multiwell PCR machine (Mastercycler, Eppendorf). Transcript abundance of the analyzed genes shown was normalized to the mean standardized expression of all six housekeeping genes listed in the primer table. We analyzed a publicly available transcriptomic dataset (GEO accession GSE63031; by Q Hao and HB Hansen, Copenhagen, Denmark) generated by deep-sequencing of transcripts isolated from murine adipose tissues [19]. Original data was downloaded, mapped and reads per kilobase per million mapped reads calculated by a dedicated software platform (Mining Station and Genome Analyzer, Genomatix).

### 2.5. Western Blot

Western blot detection of UCP1 was performed with a primary rabbit antibody raised against hamster UCP1 [20]. GMPR was detected with a rabbit polyclonal antibody raised against a peptide representing amino acids 2–16 of human GMPR, generated by Ernest Beutler (San Diego, CA, USA) and kindly provided by Reed Larsen (Boston, MA, USA) [13,21]. We detected pan-actin with a commercial mouse monoclonal antibody (MAB1501, Merck Millipore). Secondary antibodies were coupled to an infrared fluorophore (goat-anti-rabbit IRDye 800CW, 925-32210; donkey-anti-mouse 680RD, 925-68072, Licor) and visualized on an imaging system (Odyssey, Licor).

## 3. RESULTS

### 3.1. Cold exposure altered brown fat expression of purine nucleotide metabolic enzymes

Cold exposure leads to a drastic increase in guanosine monophosphate reductase (GMPR) in activated brown adipose tissue (BAT) [13]. This

enzyme converts guanosine monophosphate (GMP) into inosine monophosphate (IMP) and thereby reduces guanosine nucleotide pool size. The product IMP is a central hub in nucleotide metabolism serving both as end point of de novo synthesis and of nucleotide degradation by GMPR and its counterpart adenosine monophosphate deaminase (AMPD; AMP to IMP) (overview of nucleotide metabolism in Suppl. Fig. 1). IMP can either be re-converted into nucleotides or degraded into hypoxanthine/xanthine. We examined mRNA expression of both synthetic and degrading enzymes in BAT of differing thermogenic activity states.

We exposed mice to thermoneutrality for 2 weeks as a control condition of inactivity. In comparison, mice were either housed at room temperature (representing mild cold exposure) or exposed to 5 °C for 4 or 8 days. We were able to reproduce a much higher abundance of GMPR transcript and protein in active BAT as compared to thermoneutrality and a similar trend for the mRNA of its adenosine equivalent AMPD (Figure 1A and B). GMPR protein seems more abundant after 4 than after 8 days of cold exposure. However, total protein and total RNA content of BAT drastically increase in response to cold in a time course of several weeks [22]. Thus, total GMPR protein amount may rather remain stable. Alternatively, degradation of purine pools at the onset of cold exposure may require greater enzyme amounts than the maintenance of continued low purine levels during prolonged cold. The mRNA of enzymes synthesizing nucleotides from IMP remained unchanged except IMP dehydrogenase (IMPDH) that tended to decrease in all states of active BAT as compared to thermoneutrality.

Additionally, we analyzed a publicly available transcriptomic dataset of brown and white adipose tissues from mice exposed to room temperature or cold [19]. In a comparison of BAT to epididymal and inguinal WAT, many transcripts of nucleotide metabolism genes were much more abundant in BAT. These included GMPR, all three isoform genes of AMPD and IMPDH (Suppl. Fig. 6A and B). In accordance with our own data, GMPR expression was strongly induced upon cold exposure, while most other transcripts maintained their high expression level (Suppl. Fig. 6C and D). IMPDH transcript abundance again decreased in response to cold.

Taken together, transcripts of multiple key genes of nucleotide metabolism were much more abundant in BAT than in WAT and the adaptation of BAT to its active state led to strong expression changes of GMPR and possibly AMPD, both enzymes that control cellular purine nucleotide degradation.

### 3.2. Adrenergic activation decreased purine nucleotide pool size specifically in brown adipocytes

Uncoupling protein 1 (UCP1) mediated, non-shivering thermogenesis is initiated by a sympathetic signal to brown adipocytes. Should changes in purine nucleotide concentration assist in the activation of UCP1 by fatty acids, we expected such alterations to be adrenergically inducible and restricted to brown adipocytes. We thus chose the model of immortalized, primary brown adipocytes treated for 1 h with the  $\beta$ -adrenergic agonist isoproterenol (10  $\mu$ M) and compared it to established cell culture models representing white adipocytes and myotubes (3T3-L1 and C1C12, respectively), all of which are sensitive to  $\beta$ -adrenergic stimuli [23,24].

Fat cell lipolysis is under adrenergic control. Accordingly, cellular free fatty acid levels strongly increased upon adrenergic activation in both white and brown adipocytes, but not in myotubes (Figure 2, Suppl. Table 1). The molar sum of all fatty acids analyzed increased 9.4-fold in brown adipocytes with palmitate (C16:0) being the most abundant fatty acid. In white adipocytes, the lower 1.6-fold increase possibly reflects export of fatty acids into the medium. The massive induction of lipolysis clearly demonstrates successful initiation of the brown adipocyte thermogenic program.

In both fat cell cultures, white and brown, adrenergic stimulation led to a global loss in purine nucleotide phosphorylation (Figure 3A, Suppl. Table 2). Both ATP and GTP concentrations dropped, while AMP and GMP concentrations increased. The ATP/ADP ratio as a surrogate measure for cellular energy charge decreased (Figure 3B). None of these changes was observed in myotubes (Figure 3A and B).

Importantly, the molar sum of all purine nucleotides was maintained in white adipocytes, but not in brown adipocytes (Figure 3C). Thus, in white adipocytes, only phosphorylation state was altered while in

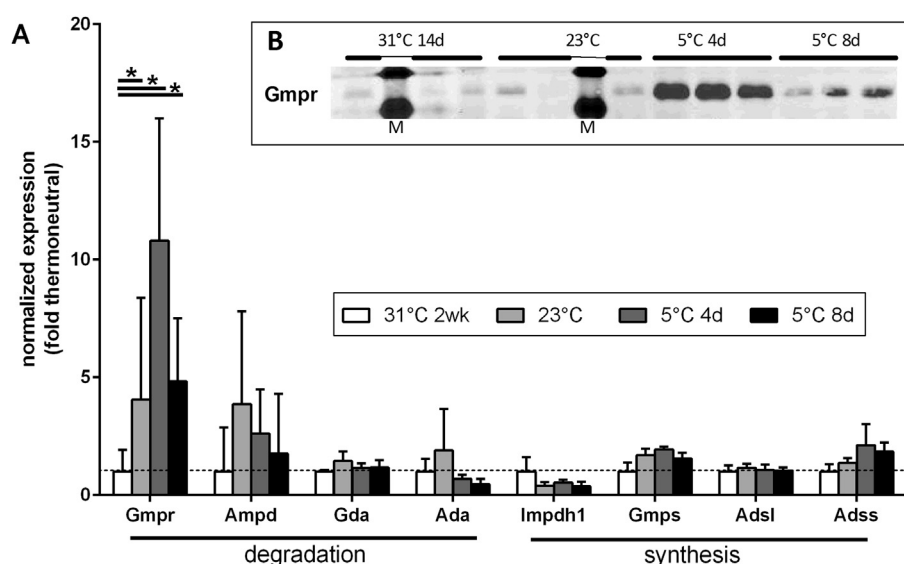


**Figure 1:** Expression of purine metabolism genes in response to varying ambient temperatures. A: Brown adipose tissue transcript abundance of mice determined by qPCR and normalized to the mean of six reference genes (see Material & Method section). Data are depicted as fold difference relative to thermoneutrality. Compared to thermoneutrality, Gmpr mRNA abundance is significantly increased by all three regimes of cold exposure while all other transcripts are not (Tukey's multiple comparisons test),  $n = 4-6$ . Inset B: Western blot detecting Gmpr protein in three of the same samples, (contralateral depot).

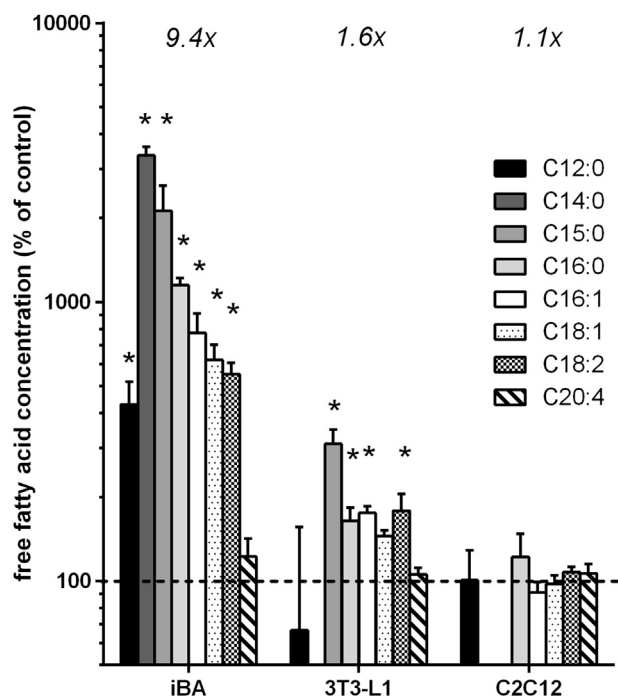


**Figure 2:** Free fatty acid levels increased upon adrenergic stimulation. Cultured cells were treated with 10  $\mu$ M isoproterenol (iso) for 1 h, lysed, and analyzed. Data are depicted as a mean percentage of control conditions  $\pm$  SD,  $n = 4$ . Significant increases are marked by a star symbol (Bonferroni corrected t-test,  $p < 0.0021$ ). Fold changes given in italics denote the absolute molar increase of all measured fatty acids upon adrenergic treatment. iBA – fully differentiated immortalized brown adipocytes, 3T3-L1 – fully differentiated white adipocytes, C2C12 – fully differentiated myotubes.

brown adipocytes, an additional loss in total pool size occurred. This decrease in purine nucleotide concentration was reflected in a similar decrease in the summed molar concentration of nucleotides inhibiting UCP1, i.e. GDP, GTP, ADP, and ATP (Figure 3C). Thus, an increase in UCP1-activating free fatty acids was accompanied by a decrease in UCP1-inhibiting nucleotides.

In accordance with a brown adipocyte specific loss of purine nucleotides, degradation products emerged in brown adipocytes, but not in white adipocytes (Figure 3A). This included IMP, the shared product of both GMP and AMP degradation by GMPR and AMPD, respectively (Figure 3A, Suppl. Fig. 1). The end products of degradation are hypoxanthine and xanthine, which can either be converted into urate or directly exported into the blood stream. Both were increased by the adrenergic stimulus specifically in brown adipocytes (Figure 3A). Further metabolites adrenergically increased were inosine and guanosine, intermediate nucleosides that can be processed to xanthine. In summary, the decrease in cellular concentration of UCP1-inhibiting nucleotides was matched by an increase in the respective intermediate and final degradation products. We replicated these key findings in freshly prepared, primary (non-immortalized) brown adipocytes with similar results (Suppl. Fig. 2).

Depending on the tissue, xanthine, hypoxanthine, or urate are end-points of nucleotide degradation. The two former can be exported into the blood for xanthine dehydrogenase catalyzed urate synthesis in the liver. We determined the concentration of purine metabolites in the supernatant medium to detect such export processes. In line with an activated purine nucleotide degradation, treatment of brown adipocytes with isoproterenol led to an increased release of hypoxanthine and xanthine into the medium (Figure 4, Suppl. Table 3). Isoproterenol

did not lead to an appearance of cytosolic proteases that would indicate an unspecific release of intracellular components (data not shown). The detected nucleotide degradation products thus represent export products of intact cells.

While myotubes displayed none of these adrenergically induced changes, white adipocytes behaved in a similar manner as brown adipocytes, albeit to a lesser extent (Figure 4, Suppl. Table 3). This observation is consistent with the decreased cellular concentration of degradation products upon adrenergic stimulation of white adipocytes (Figure 3A). Taken together, the adrenergic changes in cellular purine metabolite concentrations of brown and white adipocytes are reflected in concomitant changes in exported metabolites.

Most cellular ATPases and GTPases react with purine nucleotides complexed to divalent cations, depending on compartment, either magnesium or calcium. Conversely, the inhibition of UCP1 by purine di- and triphosphate nucleotides is exerted by the free, non-complexed form of nucleotide. We determined adrenergically induced changes in the cellular concentration of magnesium and calcium. The total cellular calcium amount increased dramatically in brown, but not in white adipocytes (Figure 5, Suppl. Table 2). Notably, the method of detection in cell lysates cannot differentiate between cellular compartments. Very high fold changes are known to occur in the cytosol of a cell, in which calcium is virtually absent in the resting state. The 15-fold increase in total cellular amount we observed, however, must have been caused by massive changes in intracellular calcium stores including the endoplasmic reticulum and mitochondria and a consequence of massive calcium uptake from the medium. Interestingly, magnesium levels do not change in parallel, although this ion is the most common divalent cation in a complex with purine nucleotides. Possibly, calcium serves multiple roles in the thermogenic response of brown adipocytes.

Taken together, treatment with the  $\beta$ -adrenergic agonist isoproterenol led to activation of lipolysis in brown and white adipocytes. Energy charge as reflected in purine nucleotide phosphorylation state was decreased. Specifically in brown adipocytes, the pool size of purine nucleotides decreased and consequently, the total amount of nucleotides inhibiting UCP1. The matching degradation products were identified in both cells and surrounding medium. A massive increase in cellular calcium is expected to even further lower the already decreased pool size of free inhibitory nucleotides.

### 3.3. Changes in purine nucleotide concentrations are required for UCP1 activation

The concentration of nucleotides inhibiting UCP1 activity decreased upon adrenergic activation by degradation and complexation. We determined possible consequences by measuring UCP1 activity in freshly prepared, primary brown adipocytes as recently described [18]. To interfere with purine metabolism, we screened the following available compounds in adrenergically induced primary brown adipocytes (main human target enzyme in parentheses): allopurinol and its active metabolite oxypurinol (xanthine dehydrogenase) [25], the research compound 1-butyl-3-methylimidazolium chloride (AMPD) [26], mycophenolic acid (IMPDH) [27] and ribavirin (IMPDH) [28]. With the exception of mycophenolic acid (MA), none of these drugs interfered with adrenergically induced loss of purine nucleotides (Suppl. Fig 3). Possibly, IMPDH inhibition by MA was effective due to its role in IMP degradation along the pathway IMP to XMP to xanthine (Suppl. Fig. 1). Alternatively, MA inhibited murine GMPR, which is highly related to IMPDH and feature similar binding constants to IMP and GMP [29]. We applied MA to disturb purine metabolism of primary brown adipocytes and functionally characterized coupled and uncoupled

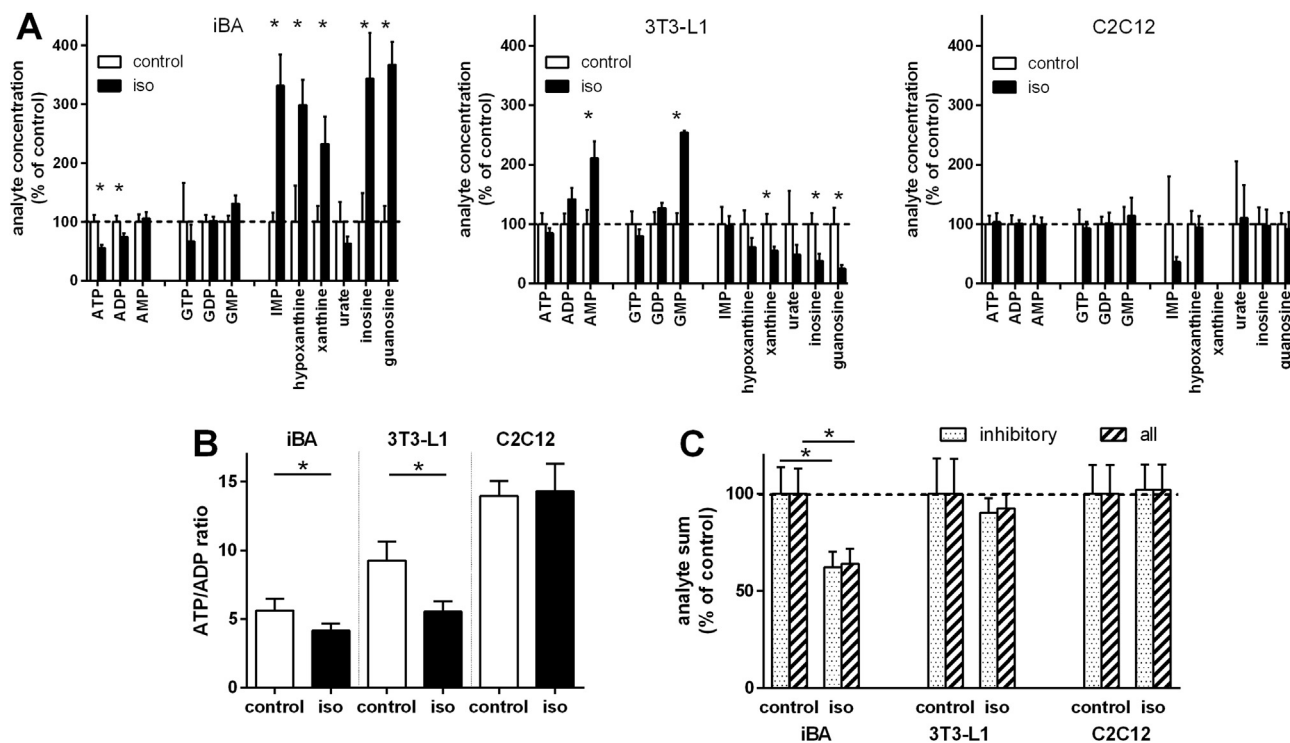


**Figure 3:** Inhibitory purine nucleotides decreased in adrenergically stimulated brown fat cells. Cultured cells were treated with 10  $\mu$ M isoproterenol (iso) for 1 h, lysed, and analyzed. A: Purine metabolite concentrations of three different cell types is depicted as mean percentage of control  $\pm$  SD,  $n = 4$ . Stars indicate a significant difference between control and isoproterenol treated cells, Holm–Bonferroni-corrected t-tests. B: Ratio between ATP and ADP  $\pm$  SD,  $n = 4$ . C: Total molar sum of all purine nucleotides (ATP, ADP, AMP, GTP, GDP, GMP) and of Ucp1 inhibiting nucleotides (ATP, ADP, GTP, GDP) as a mean percentage of control  $\pm$  SD,  $n = 4$ . Stars in B and C indicate a significant difference between control and isoproterenol treated cells,  $p < 0.05$ . iBA – fully differentiated immortalized brown adipocytes, 3T3-L1 – fully differentiated white adipocytes, C2C12 – fully differentiated myotubes.

respiration. After a phase of routine respiration, we injected the ATP synthase blocker oligomycin A to determine basal uncoupled respiration. In the presence of 2% fatty acid free bovine serum albumin, addition of isoproterenol activates UCP1-dependent uncoupled respiration. Carbonyl cyanide 4-(trifluoromethoxy)-phenylhydrazone (FCCP) stimulates maximal uncoupled respiration. The complex III inhibitor

antimycin A determines the non-mitochondrial fraction of oxygen consumption.

In this setup, brown adipocytes strongly increased respiration upon isoproterenol treatment (Figure 6A). In other words, active UCP1 uncoupled brown adipocyte mitochondria. Inhibition of IMPDH (and possibly GMPR) by MA decreased the specific respiration mediated by

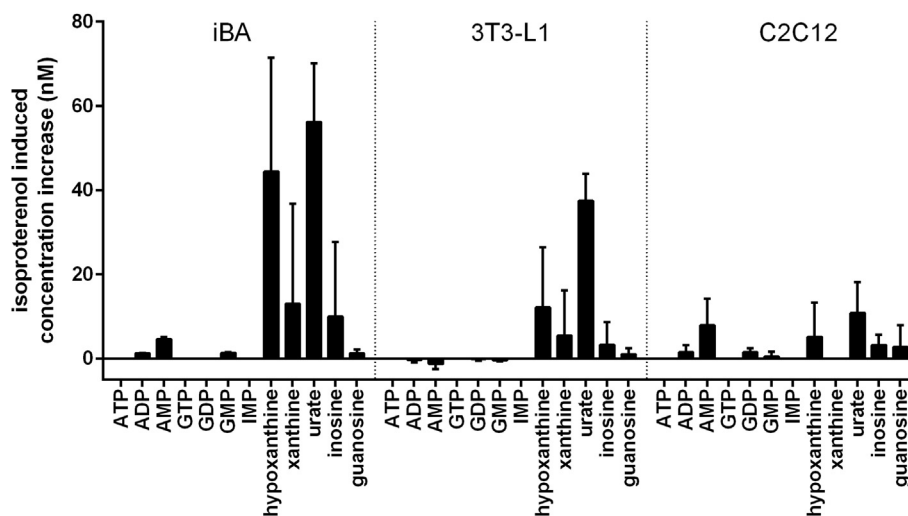


**Figure 4:** Adrenergically stimulated brown fat cells released purine nucleotide degradation products. Cultured cells were treated with 10  $\mu$ M isoproterenol for 1 h, supernatants sampled and analyzed. Purine metabolite concentration of three different cell types is depicted as absolute, isoproterenol-induced release as compared to control conditions, mean  $\pm$  SD,  $n = 4$ . iBA – fully differentiated immortalized brown adipocytes, 3T3-L1 – fully differentiated white adipocytes, C2C12 – fully differentiated myotubes.

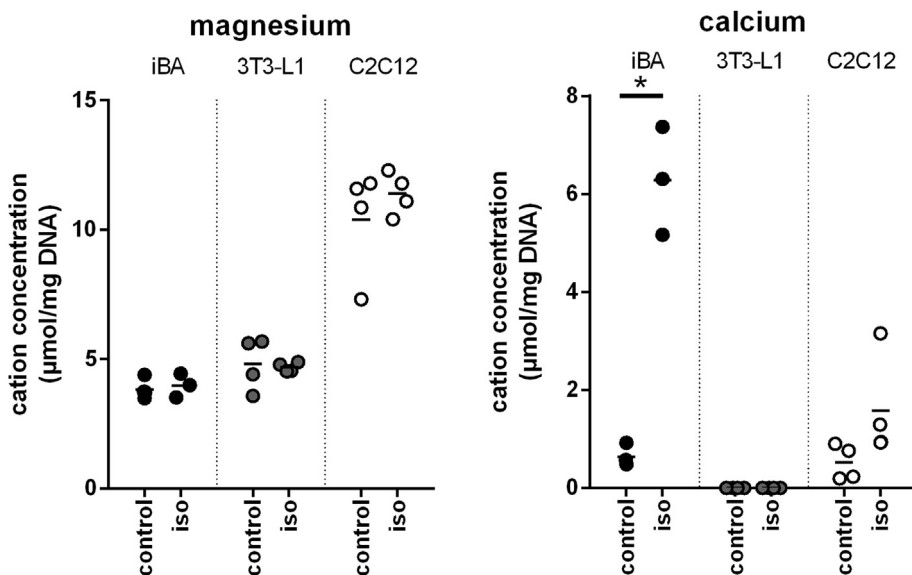


**Figure 5:** Cellular calcium increased in adrenergically stimulated brown fat cells. Cultured cells were treated with vector (control) or 10  $\mu\text{M}$  isoproterenol (iso) for 1 h, lysed and analyzed. Ion concentrations of three different cell types are depicted as a mean percentage of the vector control,  $n = 3$ . The star indicates a significant difference between control and isoproterenol treated cells,  $p < 0.05$ . iBA – fully differentiated immortalized brown adipocytes, 3T3-L1 – fully differentiated white adipocytes, C2C12 – fully differentiated myotubes.

UCP1 activity in a dose dependent manner, while maximal respiration during unspecific FCCP uncoupling was unaffected (Figure 6A and B). Accordingly, absolute oxygen consumption attributable to UCP1 activity was dose-dependently decreased by MA (Figure 6C). Thus, adrenergically induced changes in the concentration of purine nucleotides are not circumstantial, but mechanistically linked to full UCP1 activity.

### 3.4. GMP reductase is sufficient to change purine nucleotide concentrations and activate UCP1

Guanosine nucleotide pool size is reduced by GMPR, an enzyme strongly induced in active BAT. We probed the interaction of GMPR and

UCP1 in a heterologous expression system previously described [17]. A GMPR expression vector was transiently transfected into the human cell line HEK293 stably expressing murine UCP1 (UCP1-HEK) or not. The presence of GMPR on the protein level was verified by western blot (Suppl. Fig. 4).

The amount of purine nucleotides within these cells remained unchanged by the presence of GMPR in native HEK293 cells (Figure 7A and B; Suppl. Table 2). In UCP1-HEK cells, however, forced GMPR expression led to a loss in phosphorylation and in total concentration of inhibitory nucleotides in a similar fashion as observed in adrenergically induced brown adipocytes. Surprisingly, altered UCP1 activity seemed

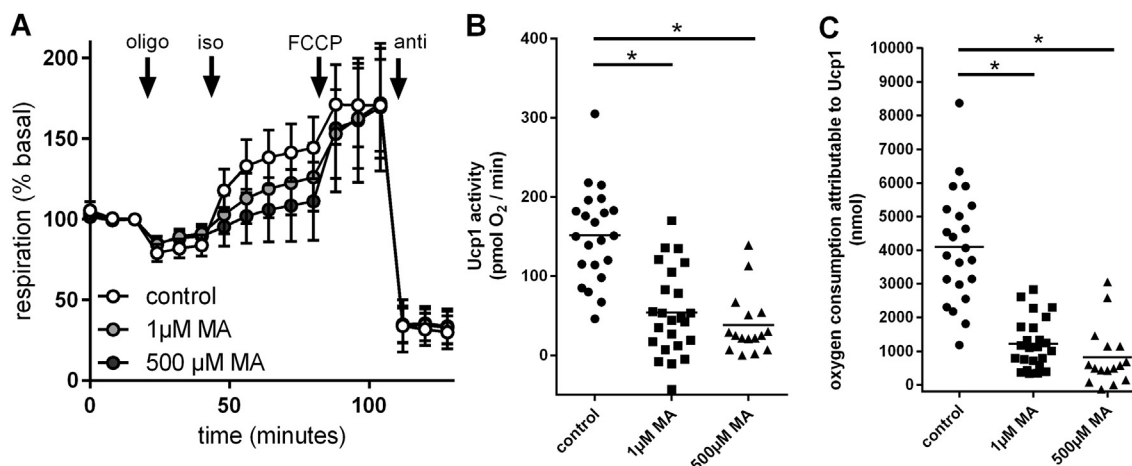


**Figure 6:** Interfering with purine degradation decreased Ucp1 activity. A – Oxygen consumption of primary brown adipocytes is represented as percentage of routine respiration in the presence of 2% bovine serum albumin. Injection of oligomycin A led to leak respiration. Isoproterenol induced Ucp1 mediated uncoupled respiration. FCCP fully uncoupled cells to maximal respiration. Antimycin A decreased oxygen consumption to a non-mitochondrial level. Mycophenolic acid was continuously present during the measurement where indicated. Depicted are mean values of 10–12 replicate wells  $\pm$  SEM. B – Respiration specifically attributable to Ucp1 activity, i.e. the maximal isoproterenol-induced increase in oxygen consumption above basal leak, as calculated from A. Treatment with 1  $\mu\text{M}$  or 500  $\mu\text{M}$  mycophenolic acid led to a significant decrease in Ucp1 activity ( $p < 0.05$ , One-way-ANOVA with Tukey post-hoc test). C – Total oxygen consumption attributable to Ucp1 activity, calculated as incremental area under the curve during the isoproterenol treatment. Treatment with 1  $\mu\text{M}$  or 500  $\mu\text{M}$  mycophenolic acid led to a significant decrease in Ucp1 activity ( $p < 0.05$ , One-way-ANOVA with Tukey post-hoc test).

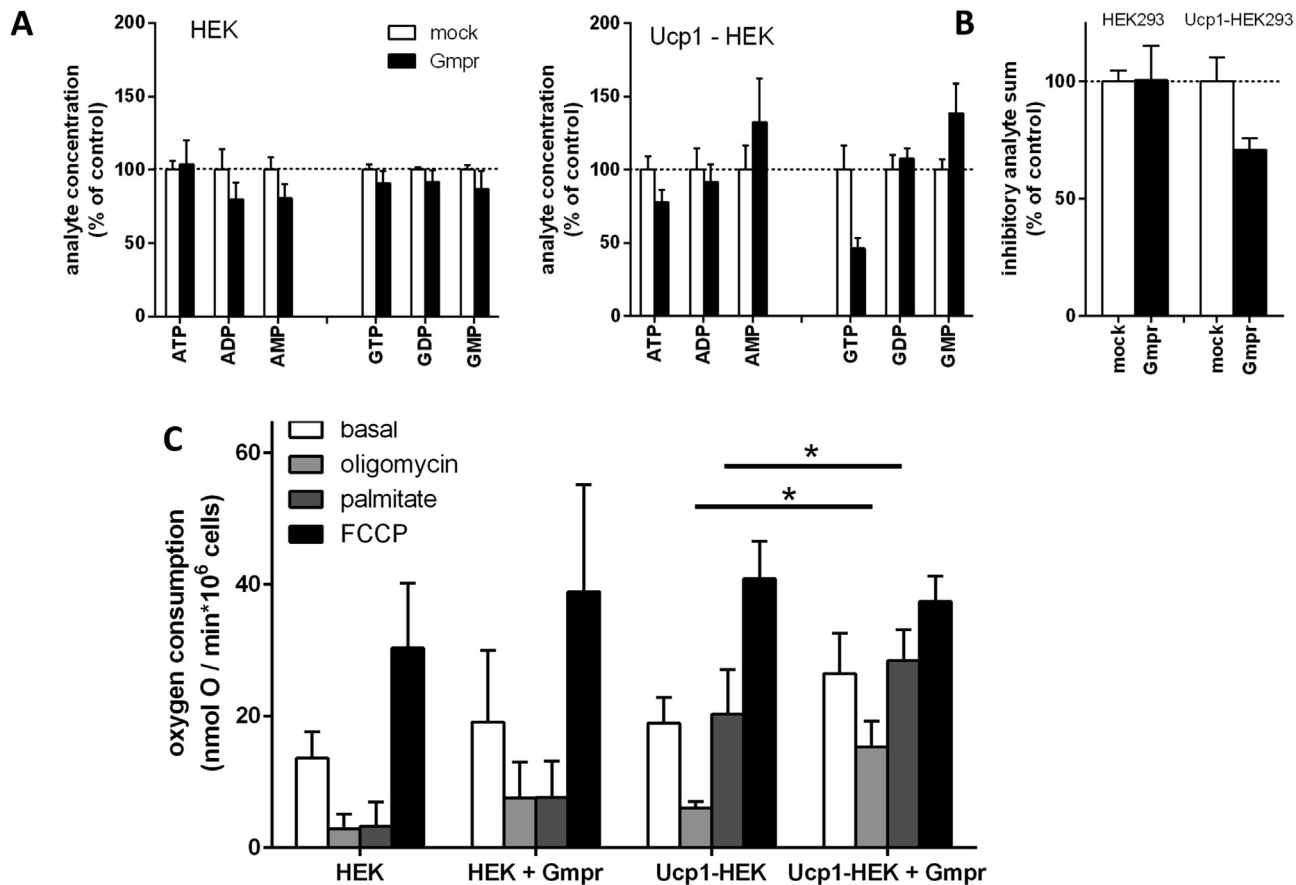


**Figure 7:** Overexpression of Gmpr increased Ucp1 activity in a heterologous system. Human embryonic kidney cells 293 (HEK) were genetically modified to stably express murine Ucp1 (Ucp1-HEK). Gmpr overexpression was performed by transient transfection of an overexpression construct. **A** – In Ucp1-Hek cells only, Gmpr expression led to a loss in phosphorylation in purine nucleotides. **B** – In Ucp1-Hek cells only, Gmpr expression led to a decrease in pool size of purine nucleotides inhibiting Ucp1, i.e. ATP, ADP, GTP and GDP. **C** – Oxygen consumption of trypsinized cells. Injection of oligomycin A (1.2  $\mu$ M) led to leak respiration. Palmitate (300  $\mu$ M) induced Ucp1 mediated uncoupled respiration. FCCP (3  $\mu$ M) fully uncoupled cells. Depicted are mean values  $\pm$  SD,  $n = 7-10$ . The effect of Gmpr transfection was assessed by 2-way-ANOVA per respiration state with cell line and transfection as factors; both factors significantly influenced all respiration states except maximal respiration with FCCP. Stars denote individual, significant Gmpr effects tested post-hoc (Sidak's multiple comparison).

not only a consequence of altered purine nucleotide concentrations but also required to bring about said alteration in the first place.

We measured basal oxygen consumption, basal leak after addition of oligomycin A, palmitate-inducible leak and maximal respiration by addition of the synthetic uncoupler FCCP (Figure 7C). A palmitate-inducible leak above basal leak specifically occurred in the presence of UCP1. In the UCP1-HEK cells, both basal and UCP1-specific leak were increased in the presence of GMPR, while native HEK293 cells remained unaffected. In this heterologous system, we reproduced an association of decreased levels of inhibitory purine nucleotides with an increase in UCP1 activity, similar to that observed in brown adipocytes.

#### 4. DISCUSSION

Non-shivering thermogenesis in brown adipose tissue (BAT) is a tightly controlled process to prevent wasting energy reserves. In the currently accepted model, regulation of uncoupling protein 1 (UCP1) activity by purine nucleotides (inhibitory) and free fatty acids (activating) serves as the central point of control (reviewed in [1]). While an adrenergically stimulated lipolytic release of free fatty acids is well established, changes in purine nucleotide pool size have not been determined in the past.

Many purine metabolites are rapidly interconvertible along complex, interwoven pathways. This is especially true for the different phosphorylation states of purine nucleotides. Thus, synthesis or elimination of GMP and AMP will consequently affect pool size of mono-, di- and triphosphate forms of these nucleotides. In both white and brown adipocytes, adrenergic activation led to a strong increase in cellular free fatty acids and at the same time to a loss of phosphorylation of purine nucleotides. Specifically in brown adipocytes, accumulated GMP and AMP were converted into the corresponding degradation products. In white adipocytes, only phosphorylation state was altered while in brown adipocytes, an additional loss in total pool size occurred. This observation is well in line with an increased activity of the enzymes GMP reductase (GMPR) and AMP deaminase (AMPD). Indeed, mRNA of both genes was more abundant in active than in inactive BAT.

Importantly, the total amount of purine nucleotides is already comparatively low in resting brown adipocytes. Purine nucleotide pool size in white adipocytes is greater by a factor of 2 and even by a factor of 6 in muscle myotubes (Suppl. Table 2). Therefore, the adrenergically induced loss of purine nucleotides by an approximate factor of 2 roughly constitutes a 10-fold difference to other tissues. This loss in total pool size was reflected in a proportional loss in UCP1-inhibitory

purine nucleotides (GDP, ADP, GTP, ATP). At the same time, a massive increase in cellular calcium amount occurred. Our measurement does not differentiate between different cellular compartments. As demonstrated previously, adrenergic stimulation of brown adipocytes leads to both calcium uptake and to intracellular mobilization of calcium stores [9–12,30]. The massive increase in cellular calcium (Figure 4) can thus be expected to be at least partially reflected in increased cytosolic calcium level. The absence of concomitant changes in magnesium levels indicates additional, specific functions of calcium. Beyond nucleotide complexation, calcium may also be involved in other metabolic processes, e.g. thermogenic futile cycling, as suggested to occur in beige adipocytes [31].

The increase in cytosolic pH in activated brown adipocytes not only decreases affinity of purine nucleotides to UCP1 but also increases complex formation of purine nucleotides with magnesium [8,32]. Already under standard conditions, less than 10% of cytosolic purine nucleotides are non-complexed to magnesium and therefore available for UCP1 inhibition [32,33]. For these reasons, the 2-fold decrease in purine nucleotides from 1/2 to 1/4 of white adipocyte concentrations (and from 1/8 to 1/16 of myotube concentrations) must be greater by far on the level of non-complexed (i.e. inhibitory) nucleotides.

In resting skeletal muscle, the cytosolic ATP concentration is in the range of 1–10 mM [34]. Based on the above assumptions, that estimate translates into 62.5–625  $\mu$ M total ATP in active brown adipocytes, of which less than 5–50  $\mu$ M are non-complexed. Adding ADP, GTP and GDP will approximatively double the total concentration of inhibitory free purine nucleotides to 10–100  $\mu$ M. The half-maximal inhibition constant of purine nucleotides acting on UCP1 has been estimated to be in precisely that range with 80  $\mu$ M at pH 7.5 and 12% molar membrane cardiolipin content [3].

Interestingly, the phenomenon of enzymatic purine nucleotide depletion has long been known for another tissue with very high metabolic activity, contracting skeletal muscle [35]. Here, millimolar changes in ATP concentration are not accompanied by equivalent changes in ADP or AMP. The loss in total adenine nucleotides is explained by the action of AMP deaminase and AMP dephosphorylase [36,37]. In this setting, the degradation of nucleotides has been interpreted to be vital to preserve the ATP/ADP ratio (and thus Gibb's free energy of ATP hydrolysis) in the face of falling ATP levels. To distinguish a role in UCP1 activation from this model, in which purine nucleotide degradation is an end in itself, we interfered in purine metabolism with mycophenolic acid (MA), an inhibitor of IMPDH. IMPDH and GMPR are highly related proteins with similar binding constants to their substrates. Inhibition of GMPR by MA thus seems plausible [29]. Alternatively, IMPDH may be important to degrade IMP along the pathway IMP to XMP to xanthine (Suppl. Fig. 1). In any case, MA to some extent prevented adrenergically induced loss of UCP1-inhibiting nucleotides. Isoproterenol induced UCP1 activity was drastically lower as determined in a proven setup [18,38]. Thus, purine metabolic remodeling is essential for maximal UCP1 activity and not a sole byproduct of another biophysical purpose.

It remains to be demonstrated that the mechanism elaborated in a model of cultured brown adipocytes is in fact present in brown fat *in vivo*. In preliminary experiments, we were unable to preserve plausible *in situ* snapshots of metabolite concentrations in murine brown adipose tissue, probably owing to very fast changes following the death of an animal. Assuming that these are mostly restricted to loss of phosphorylation, the cumulative concentration of ATP + ADP + AMP and GTP + GDP + GMP may still be informative. While adenine nucleotide pool size was inconclusive, guanine nucleotides were clearly less in abundant in interscapular BAT compared to inguinal WAT and were subject to further

degradation after 24 h of cold exposure (5 °C, Suppl. Fig. 5). In the future, we will assess the applicability of freeze-clamping to preserve nucleotide levels in adipose tissues harvested from pentobarbital-anesthetized mice [39,40].

In the heterologous cell system HEK293, GMPR and UCP1 expression alone were sufficient to alter purine nucleotide levels. Reduced amounts of nucleotides inhibiting UCP1 were associated with increased UCP1 activity. Therefore, both interfering in purine nucleotide depletion in brown adipocytes and conversely causing them in HEK293 cells led to the corresponding change in UCP1 activity. We conclude that purine nucleotide depletion is involved in the regulation of the activity of thermogenic UCP1. This may provide a mechanistic base for the very recent finding that UCP1 mediated thermogenesis can occur in the absence of lipolysis [41,42].

## CONFLICT OF INTEREST

On behalf of all authors I declare the absence of any conflicts of interest.

## ACKNOWLEDGMENTS

The study was supported by the Else Kröner-Fresenius-Stiftung and the German Research Foundation (grant KL 973/12-1). Publication was supported by the German Research Foundation (DFG) and the Technical University of Munich within the funding programme Open Access Publishing.

## APPENDIX A. SUPPLEMENTARY DATA

Supplementary data related to this article can be found at <https://doi.org/10.1016/j.molmet.2017.12.010>.

## REFERENCES

- [1] Klingenspor, M., Bast, A., Bolze, F., Li, Y., Maurer, S., Schweizer, S., et al., 2017. Brown adipose tissue. In: Symonds, M.E. (Ed.), *Adipose tissue biology*. Cham: Springer International Publishing. p. 91–147.
- [2] Klingenberg, M., Winkler, E., 1985. The reconstituted isolated uncoupling protein is a membrane potential driven H<sup>+</sup> translocator. *The EMBO Journal* 4(12):3087–3092.
- [3] Klingenberg, M., 2009. Cardiolipin and mitochondrial carriers. *Biochim Biophys Acta* 1788(10):2048–2058.
- [4] Jezek, P., Houstek, J., Drahotka, Z., 1988. Alkaline pH, membrane potential, and magnesium cations are negative modulators of purine nucleotide inhibition of H<sup>+</sup> and Cl<sup>-</sup> transport through the uncoupling protein of brown adipose tissue mitochondria. *Journal of Bioenergetics and Biomembranes* 20(5):603–622.
- [5] Goubern, M., Chapey, M.F., Senault, C., Laury, M.C., Yazbeck, J., Miroux, B., et al., 1992. Effect of sympathetic de-activation on thermogenic function and membrane lipid composition in mitochondria of brown adipose tissue. *Biochimica et Biophysica Acta* 1107(1):159–164.
- [6] Senault, C., Yazbeck, J., Goubern, M., Portet, R., Vincent, M., Gallay, J., 1990. Relation between membrane phospholipid composition, fluidity and function in mitochondria of rat brown adipose tissue. Effect of thermal adaptation and essential fatty acid deficiency. *Biochimica et Biophysica Acta* 1023(2):283–289.
- [7] Klingenberg, M., 1988. Nucleotide binding to uncoupling protein. Mechanism of control by protonation. *Biochemistry* 27(2):781–791.
- [8] Chinet, A., Friedli, C., Seydoux, J., Girardier, L., 1978. Does cytoplasmic alkalization trigger mitochondrial energy dissipation in the brown adipocyte? *Experientia Supplementum* 32:25–32.



- [9] Hayato, R., Higure, Y., Kuba, M., Nagai, H., Yamashita, H., Kuba, K., 2011. Beta(3)-Adrenergic activation of sequential Ca(2+) release from mitochondria and the endoplasmic reticulum and the subsequent Ca(2+) entry in rodent brown adipocytes. *Cell Calcium* 49(6):400–414.
- [10] Wilcke, M., Nedergaard, J., 1989. Alpha 1- and beta-adrenergic regulation of intracellular Ca2+ levels in brown adipocytes. *Biochemical and Biophysical Research Communications* 163(1):292–300.
- [11] Nedergaard, J., 1981. Effects of cations on brown adipose tissue in relation to possible metabolic consequences of membrane depolarisation. *European Journal of Biochemistry* 114(1):159–167.
- [12] Connolly, E., Nanberg, E., Nedergaard, J., 1984. Na+-dependent, alpha-adrenergic mobilization of intracellular (mitochondrial) Ca2+ in brown adipocytes. *European Journal of Biochemistry* 141(1):187–193.
- [13] Salvatore, D., Bartha, T., Larsen, P.R., 1998. The guanosine monophosphate reductase gene is conserved in rats and its expression increases rapidly in brown adipose tissue during cold exposure. *Journal of Biological Chemistry* 273(47):31092–31096.
- [14] Watanabe, M., Yamamoto, T., Kakuhata, R., Okada, N., Kajimoto, K., Yamazaki, N., et al., 2008. Synchronized changes in transcript levels of genes activating cold exposure-induced thermogenesis in brown adipose tissue of experimental animals. *Biochimica et Biophysica Acta* 1777(1):104–112.
- [15] Li, Y., Bolze, F., Fromme, T., Klingenspor, M., 2014. Intrinsic differences in BRITe adipogenesis of primary adipocytes from two different mouse strains. *Biochimica et Biophysica Acta*.
- [16] Uldry, M., Yang, W., St-Pierre, J., Lin, J., Seale, P., Spiegelman, B.M., 2006. Complementary action of the PGC-1 coactivators in mitochondrial biogenesis and brown fat differentiation. *Cell Metabolism* 3(5):333–341.
- [17] Jastroch, M., Hirschberg, V., Klingenspor, M., 2012. Functional characterization of UCP1 in mammalian HEK293 cells excludes mitochondrial uncoupling artefacts and reveals no contribution to basal proton leak. *Biochimica et Biophysica Acta* 1817(9):1660–1670.
- [18] Li, Y., Fromme, T., Schweizer, S., Schottl, T., Klingenspor, M., 2014. Taking control over intracellular fatty acid levels is essential for the analysis of thermogenic function in cultured primary brown and brite/beige adipocytes. *EMBO Reports* 15(10):1069–1076.
- [19] Hao, Q., Yadav, R., Basse, A.L., Petersen, S., Sonne, S.B., Rasmussen, S., et al., 2015. Transcriptome profiling of brown adipose tissue during cold exposure reveals extensive regulation of glucose metabolism. *American Journal of Physiology – Endocrinology and Metabolism* 308(5):E380–E392.
- [20] Meyer, C.W., Korthaus, D., Jagla, W., Cornali, E., Grosse, J., Fuchs, H., et al., 2004. A novel missense mutation in the mouse growth hormone gene causes semidominant dwarfism, hyperghrelinemia, and obesity. *Endocrinology* 145(5):2531–2541.
- [21] Beutler, E., Gelbart, T., Kuhl, W., 1990. Human red cell glucose-6-phosphate dehydrogenase: all active enzyme has sequence predicted by the X chromosome-encoded cDNA. *Cell* 62(1):7–9.
- [22] Jacobsson, A., Muhleisen, M., Cannon, B., Nedergaard, J., 1994. The uncoupling protein thermogenin during acclimation: indications for pre-translational control. *American Journal of Physiology* 267(4 Pt 2):R999–R1007.
- [23] Frost, R.A., Nystrom, G.J., Lang, C.H., 2004. Epinephrine stimulates IL-6 expression in skeletal muscle and C2C12 myoblasts: role of c-Jun NH2-terminal kinase and histone deacetylase activity. *American Journal of Physiology – Endocrinology and Metabolism* 286(5):E809–E817.
- [24] Miller, C.N., Yang, J.Y., England, E., Yin, A., Baile, C.A., Rayalam, S., 2015. Isoproterenol increases uncoupling, glycolysis, and markers of beigeing in mature 3T3-L1 adipocytes. *PLoS One* 10(9):e0138344.
- [25] Yue, T.F., Gutman, A.B., 1964. Effect of allopurinol (4-Hydroxypyrazolo-(3,4-D) Pyrimidine) on serum and urinary uric acid in primary and secondary gout. *The American Journal of Medicine* 37:885–898.
- [26] Skladanowski, A.C., Stepnowski, P., Kleszczynski, K., Dmochowska, B., 2005. AMP deaminase in vitro inhibition by xenobiotics A potential molecular method for risk assessment of synthetic nitro- and polycyclic musks, imidazolium ionic liquids and N-glucopyranosyl ammonium salts. *Environmental Toxicology and Pharmacology* 19(2):291–296.
- [27] Allison, A.C., Eugui, E.M., 2000. Mycophenolate mofetil and its mechanisms of action. *Immunopharmacology* 47(2–3):85–118.
- [28] Hedstrom, L., 2009. IMP dehydrogenase: structure, mechanism, and inhibition. *Chemical Reviews* 109(7):2903–2928.
- [29] Hedstrom, L., 2012. The dynamic determinants of reaction specificity in the IMPDH/GMPR family of (beta/alpha)(8) barrel enzymes. *Critical Reviews in Biochemistry and Molecular Biology* 47(3):250–263.
- [30] Connolly, E., Nedergaard, J., 1988. Beta-adrenergic modulation of Ca2+ uptake by isolated brown adipocytes. Possible involvement of mitochondria. *Journal of Biological Chemistry* 263(22):10574–10582.
- [31] Ikeda, K., Kang, Q., Yoneshiro, T., Camporez, J.P., Maki, H., Homma, M., et al., 2017. UCP1-independent signaling involving SERCA2b-mediated calcium cycling regulates beige fat thermogenesis and systemic glucose homeostasis. *Nature Medicine* 23(12):1454–1465.
- [32] Luthi, D., Gunzel, D., McGuigan, J.A., 1999. Mg-ATP binding: its modification by spermine, the relevance to cytosolic Mg2+ buffering, changes in the intracellular ionized Mg2+ concentration and the estimation of Mg2+ by 31P-NMR. *Experimental Physiology* 84(2):231–252.
- [33] Corkey, B.E., Duszynski, J., Rich, T.L., Matschinsky, B., Williamson, J.R., 1986. Regulation of free and bound magnesium in rat hepatocytes and isolated mitochondria. *Journal of Biological Chemistry* 261(6):2567–2574.
- [34] Kushmerick, M.J., Moerland, T.S., Wiseman, R.W., 1992. Mammalian skeletal muscle fibers distinguished by contents of phosphocreatine, ATP, and Pi. *Proceedings of the National Academy of Sciences of the United States of America* 89(16):7521–7525.
- [35] Parnas, J.K., 1929. Über die Ammoniakbildung im Muskel und ihren Zusammenhang mit Funktion und Zustandsänderung. VI. Mitteilung: der Zusammenhang der Ammoniakbildung mit der Umwandlung des Adeninnucleotids zu Inosinsäure. *Biochemische Zeitschrift*(206):16–38.
- [36] Sahlin, K., Broberg, S., 1990. Adenine nucleotide depletion in human muscle during exercise: causality and significance of AMP deamination. *International Journal of Sports Medicine* 11(Suppl 2):S62–S67.
- [37] Hancock, C.R., Brault, J.J., Terjung, R.L., 2006. Protecting the cellular energy state during contractions: role of AMP deaminase. *Journal of Physiology & Pharmacology* 57(Suppl 10):17–29.
- [38] Li, Y., Fromme, T., Klingenspor, M., 2016. Meaningful respirometric measurements of UCP1-mediated thermogenesis. *Biochimie*.
- [39] Palladino, G.W., Wood, J.J., Proctor, H.J., 1980. Modified freeze clamp technique for tissue assay. *Journal of Surgical Research* 28(2):188–190.
- [40] Ohlson, K.B., Lindahl, S.G., Cannon, B., Nedergaard, J., 2003. Thermogenesis inhibition in brown adipocytes is a specific property of volatile anesthetics. *Anesthesiology* 98(2):437–448.
- [41] Schreiber, R., Diwoky, C., Schoiswohl, G., Feiler, U., Wongsiriroj, N., Abdellatif, M., et al., 2017. Cold-induced thermogenesis depends on ATGL-mediated lipolysis in cardiac muscle, but not brown adipose tissue. *Cell Metabolism*.
- [42] Shin, H., Ma, Y., Chanturiya, T., Cao, Q., Wang, Y., Kadegowda, A.K.G., et al., 2017. Lipolysis in brown adipocytes is not essential for cold-induced thermogenesis in mice. *Cell Metabolism*.